Flood meteorology, hydrology, and geomorphology of the Upper Godavari River, Western India

Archana D. Patil[1], Pramodkumar S. Hire[2], Gitanjali W. Bramhankar[3], Rajendra P. Gunjal[4], Vitthal K. Anwat[5]

[1]RNC Arts, JDB Commerce and NSC Science College, Nashik 422101, India

[2,3]HPT Arts and RYK Science College, Nashik 422005, India

[4]KRT Arts, BH Commerce and AM Science College, Nashik 422002, India

[5]K.S.K.W. Arts, Science & Commerce College, Nashik 422008, India

Priti R. Khandare[6]

[6]Satish Pradhan Dnyansadhana College, Thane 400604, India

Abstract

Meteorological, hydrological, and geomorphological aspects of large floods on the Upper Godavari River were investigated. Synoptic conditions associated with large floods were analyzed to gain an understanding of flood hydrometeorology in the basin. The study reveals that the southwest summer monsoon dominates rainfall in the Upper Godavari Basin (90% of annual rainfall). Moreover, interannual variability was characterized by increased frequency and magnitude of floods primarily after the 1930s and the majority of large floods were connected with low-pressure systems. Unit discharges (Q_u) and flash-flood magnitude index (*FFMI*) were computed to understand the potential for large floods. The high Q_u (1.13 and 6.00 m³ s⁻¹ km⁻²) are likely to be effective in terms of geomorphic changes in the channel. The greater *FFMI* values (0.27 and 0.56) indicate the flashy and variable nature of floods and the possibility of significant geomorphic work. Parameters of flood hydraulics and hydrodynamics were computed to estimate the efficacy of infrequent and large-magnitude floods. The highest values for unit stream power (5909.61 W m⁻²) and bed shear stress (609 N m⁻²) reveal the unusually high capacity of the river to erode and transport coarse sediments. The Froude numbers (>1) confirm extremely erosive supercritical flows. High Reynolds numbers indicate exceedingly turbulent flood discharges, capable of accomplishing a variety of geomorphic activities.

1. Introduction

India lies at the heart of the classical monsoon region; it is extremely vulnerable to frequent hazards of floods and intense downpours that accompany low-pressure systems (LPS) during the monsoon season (Kale et al. 1994). Such massive floods are critical events, from the standpoint of human impact as well as in terms of geomorphic effectiveness.

The Godavari River has one of the most potent flood regimes in the seasonal tropics (Khandare 2009). Major flood events have been reported for the Godavari River, for instance, in September 1969 (Mujumdar et al. 1970), August 1981 (Pandharinath 1984), August 2006, September 2008 (Khandare 2009) and August 2019. However, information is scant about the causes and effects of such large floods on the Upper Godavari River (UGR). Therefore, the objectives of this paper are to examine the meteorological aspects of large floods, to understand the hydrological characteristics of floods, and to evaluate the geomorphic impacts of floods on the UGR in terms of hydraulic properties and effects.

2. Upper Godavari Basin (UGB): geomorphic setting

The Godavari River, with 1465 km, is the second longest river in India and the longest among all the rivers in peninsular India. The river rises in the Western Ghat at Bramhagiri near Trimbakeshwar at an elevation of 1287 m in the Nashik District of Maharashtra State (Fig. 1). The river discharges into the Bay of Bengal at Narasapuram in the West Godavari district of the Andhra Pradesh. The total drainage area of the Godavari Basin is 312,813 km². This study represents an attempt to comprehend the meteorological, hydrological, and geomorphological aspects of large floods of the Upper Godavari River (UGR) in the headwater region (UGB = 5085 km²), i.e., from the river's source to Kopargaon Tehsil. The UGB is bounded by the Satmala Range in the north, the Western Ghat Escarpment in the west and the Kalsubai Range in the south. Geologically, the region is underlain by Cretaceous-Eocene Deccan Trap basalt; there are no later formations except the older alluvium of the late Pleistocene (Mujumdar et al. 1970) to late Holocene (Kale 2022). The major tributaries of the Upper Godavari River (UGR) are Darna, Dev, and Umri on the right bank, and Kadva, and Goi on the left bank.
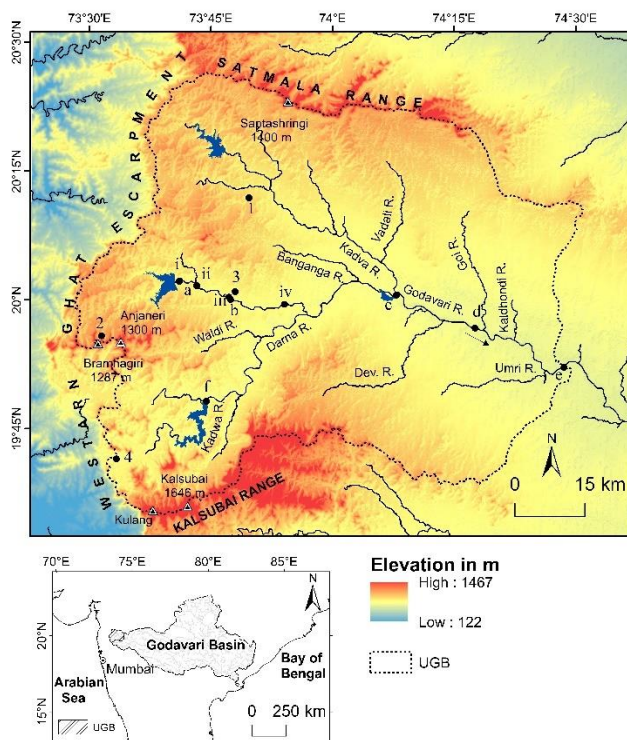

Fig. 1. Physiographic map of the study area: (1) Dindori, (2) Trimbakeshwar, (3) Nashik, (4) Igatpuri; (a) Gangapur Dam, (b) Nashik, (c) Nandur Madmeshwar Dam, (d) Chass, (e) Kopargaon, (f) Darna Dam; (i) Dugaon; (ii) Someshwar, (iii) Sarkarwada, (iv) Odha; UGB – Upper Godavari River.

3. Data source

Rainfall data from four rain gauge stations in the UGB were employed: Dindori, Trimbakeshwar, Nashik, and Igatpuri, with records ranging from 119 to 143 years (1878 to 2019). The data were collected from the India Meteorological Department (IMD), Pune. Data for tracks of low-pressure systems (LPS) from 1891 to 2019 were derived from the e-atlas obtained from IMD, Chennai. The annual maximum series (AMS)

stage data were procured from the Centre Water Commission (CWC), New Delhi, Maharashtra Engineering Research Institute (MERI) and Hydrology Department, Nashik, for five gauging sites on the UGR and one site on its tributary, i.e., the Darna River. The AMS gauge records for the UGR are short and discontinuous (24 to 50 years). The cross-sectional surveys were carried out at four sites to compute parameters of hydraulics and hydrodynamics with respect to high flood levels (HFL).

4. Flood meteorology

Rainfall characteristics in monsoonal regions, particularly the distribution in space and time, are important in terms of flood generation. Consequently, one of the core objectives of this paper is to analyze the meteorological data that are currently available and to pinpoint the characteristics of rainfall that lead to significant flooding on the UGB. The UGR is rainfed, as are its tributaries. The southwest monsoon season's heavy to extremely severe rainfall is therefore responsible for all flooding on the river. Excessive and widespread rainfall is caused by a range of flood-producing meteorological conditions. These include LPS originating over the Bay of Bengal and terrestrial depressions, along with active to vigorous monsoon activity. In the following section, the features of flood-generating rainfall and allied synoptic situations are depicted. The UGB is located in an environment typical of southwestern monsoonal tropics, with periodic large-magnitude rainfall. The UGB receives 1780 mm of rain on average per year, with monsoon months, i.e., mid-June to early October, accounting for 90% of the total annual rainfall. The rainiest month is July, followed by August; they contribute 37% and 27% of the basin's total annual rainfall, respectively.

4.1. Interannual rainfall variability and associated floods

Akin to other monsoon-dominated rivers of India, the UGB also shows significant interannual variation in rainfall and, therefore, flood events. Table 1 lists details of the four stations with long-duration rainfall records (>100 years; between 1878 and 2019). Mean annual rainfall of the UGB ranges from 716 mm at Nashik to 3241 mm at Igatpuri. The low coefficient of variation (C_v) (24-33%) of annual rainfall in most parts of the basin demonstrates that interannual variability is not particularly high. The annual rainfall at each site varies greatly (Table 1). For example, the minimum annual rainfall at Nashik was 332 mm in 1984, whereas the maximum annual rainfall at Igatpuri was 6601 mm in 1931.

Table 1. Annual rainfall characteristics of selected stations in the Upper Godavari Basin (UGB) (from 1878 to 2019). Data source: IMD.

Site	Altitude (m ASL)	Record length (years)	*Rmax* (mm) [year]	*Rmin* (mm) [year]	*AAR* (mm)	σ	*Cs*	*Cv*
Dindori	649	142	1820 [2017]	348 [1986]	791	240	1.17	0.30
Igatpuri	609	140	6601 [1931]	1463 [2015]	3241	772	0.56	0.24
Nashik	593	143	1540 [1883]	332 [1984]	716	234	0.78	0.33
Trimbakeshwar	715	119	4368 [1917]	935 [1998]	2373	574	0.41	0.24

Rmax – maximum rainfall; ASL – above sea level; *Rmin* – minimum rainfall; *AAR* – average annual rainfall; σ – standard deviation; *Cs* – coefficient of skewness; *Cv* – coefficient of variation. See Fig. 1 for site locations.

The coefficient of skewness (C_S) values range from 0.41 to 1.17 and are positive for all of the stations. The Dindori site reveals a relatively high positive C_S value. The positive C_S values indicate episodes of one or two or a few very wet years during the gauged period, for instance, in 1813 (1376 mm), 1981 (1600 mm), 2019 (1371 mm) and 2017 (1819 mm). Given that C_S values have been established based on more than 100 years of data, they are all statistically significant (Viessman et al. 1989).

The interannual variability of rainfall is shown as a time series plot in Figure 2 for the rain gauge sites located in UGB. The figure reveals that previous to 1930, rainfall was commonly below average with low interannual variability. In contrast, in many years between 1930 and 1980, above-average annual rainfall was recorded, with high interannual variability. After 1980, rainfall was frequently below average, with moderate interannual variability. In particular, after the 1930s, interannual variability was marked by an increase in the frequency and magnitude of floods on the UGR. Interestingly, similar results and remarkable interannual variability in the rainfall totals have been reported for some of the westward-flowing rivers of India (Kale 1999; Hire 2000; Patil 2018; Pawar, Hire 2018; Pawar 2019; Patil, Hire 2020; Anwat 2022). The time series plot of interannual variability of rainfall and associated floods shows that almost all of the large flood events in the UGR have occurred when rainfall was above average (Fig. 2). To identify the flood years for the UGR, the annual rainfall and discharge data were analyzed by applying equation 1 (Pant, Kumar 1997) and equation 2.

$$Ri \geq AAR + 1\sigma \tag{1}$$

where: Ri is the rainfall of year i, AAR is the long-term mean rainfall, and σ is the standard deviation.

$$Qi \geq Qm + 1\sigma \tag{2}$$

where: Qi is the discharge of year i, and Qm is the mean annual peak discharge.
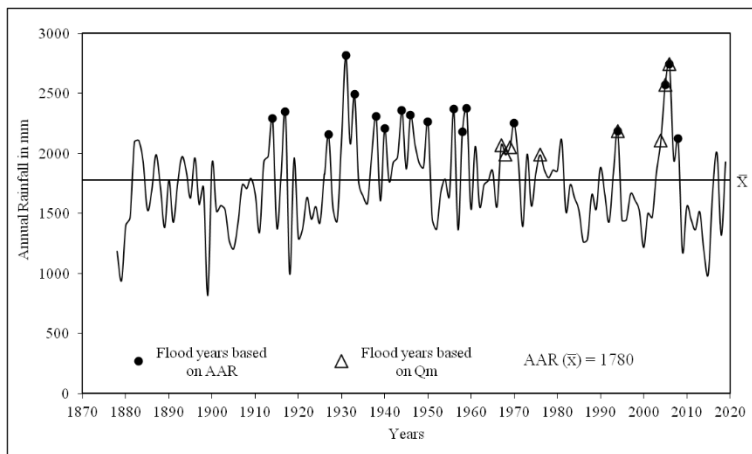

Fig. 2. Interannual rainfall variability and associated floods, UGR (1878 to 2019); AAR =annual average rainfall; Qm = mean annual peak discharge.

4.2. Characteristics of the flood-generating low-pressure systems (LPS)

During all months of the year, except February, the Indian subcontinent is subjected to cyclonic disturbances (such as depressions and cyclonic storms) (Dhar et al. 1984). Attributable to the heavy rainfalls associated with these cyclonic disturbances, floods occur in those rivers whose catchments drain the rainstorm area (Dhar et al. 1984). These floods mark the largest recorded peaks in a flood time series (Kale et al. 1994). Flood-producing rainstorms are associated with Bay of Bengal depressions moving westward, general active monsoon conditions over Madhya Pradesh and Gujarat, and terrestrial depressions, according to earlier and more recent studies of the synoptic conditions associated with rainstorms (Abbi, Jain 1971; Ramaswamy 1987; Hire 2000; Patil 2018; Pawar 2019).

An effort has been made to identify and analyze the LPS tracks that caused the highest discharges in the basin to understand the relationship between LPS and floods in the UGB. The e-Atlas software was used to locate the LPS tracks, and ArcGIS 9.3 was applied to analyze them. The buffer zone was delineated at 500 km from the basin margin, and only LPS tracks that passed through the buffer zone were chosen for the investigation (Patil, Hire 2020) (Fig. 3). According to an assessment of the synoptic conditions associated with the flood-generating LPS, several of the LPS in the UGB were the result of Bay depressions and active monsoon conditions over central India. The association of LPS and consequent floods of the UGB were studied by using the AMS data. Streamflow records available for some sites on the UGR and its tributaries indicate that the LPS can have an immense impact. The systems, which comprise lows, depressions, and cyclonic storms (Dhar, Nandargi 1995), cause extreme stream rise, leading to large floods. Table 2 confirms the prevalence of LPS-linked floods in the UGR in August or September, by which time an average of ~42% of the annual rainfall has been received, and soils are completely saturated, further increasing the magnitude of floods.
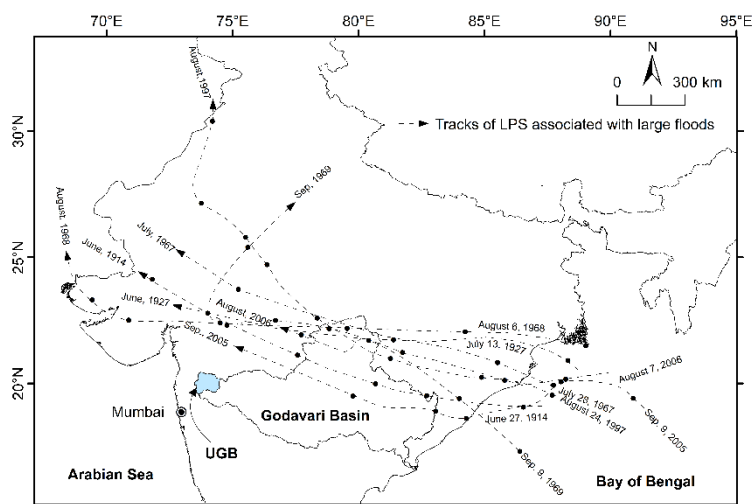

Fig. 3. Tracks of LPS associated with large floods on the UGR (1891 to 2019).

In the quadrants to the right of the depression track, the rainfall field is flat. Conversely, large gradients of rainfall subsist in the left quadrants, especially along and west of 80°E. Additionally, the area with the

maximum rainfall is in the left front quadrant, 150 km from the center and 50 to 150 km from the depression track (Mooley 1973). The position of the UGB remained in the left front quadrant during transit of the bulk of LPS(s) that traveled WNW or NW (Fig. 3; Table 2), thus resulting in high-magnitude floods. For instance, in 2005 and 2006, LPS caused high flood levels ($Qi \geq Qm + 1\sigma$ at Nashik; 633 m³ s⁻¹) on the UGR with 941 and 1034 m³ s⁻¹ discharges, respectively, at the Nashik gauging station. We investigated the relationship between LPS, greatest 24-hr. rainfall, and large floods in the UGB. The highest 24-hr. rainfall at Nashik station was associated with LPS (Table 3). The September 10, 1969, LPS, which transited from the northwest corner of the UGB, is an excellent example of this kind (Fig. 3). The 24-hr. rainfall measured at Nashik station was 183 mm (16% of the total annual rainfall) (Table 3).

Table 2. Synoptic conditions associated with major floods on the Upper Godavari River.

Month, date and year of flood	Annual rainfall in the basin (mm)	Monsoon rainfall in the basin (mm)	Associated LPS
July 28, 1967	2071 (+16.37%)	1966 (+10.46%)	Bay Depression
August 6, 1968	1990 (+11.80%)	1880 (+05.64%)	Bay Depression
September 9, 1969	2053 (+15.33 %)	1984 (+11.48%)	Bay Depression
August 23, 1997	1664 (–06.49%)	1580 (–11.25%)	Bay Depression
September 23, 2005	2569 (+44.35%)	2481 (+39.39%)	Bay Depression
August 08, 2006	2744 (+54.18%)	2624 (+47.42%)	Bay Depression

Values in brackets represent percentage departure from the mean.

Table. 3 Low-pressure systems and highest 24 hr. rainfall at Nashik station. Data source IMD.

Date	Highest rainfall (mm)	Annual rainfall (mm)	Average annual rainfall (mm) 1878-2019	% of annual rainfall
June 26, 1984	118	999	715	12
July 13, 1927	86	798	715	11
Sept. 10, 1969	183	1145	715	16
Sept.22, 2005	109	1267	715	09
August 8, 2006	114	1233	715	09

5. Flood hydrology

The UGR, similar to other monsoonal rivers of peninsular India, is also subjected to high-magnitude floods at regular intervals. Therefore, it is of paramount importance to know the hydrologic characteristics of floods in terms of magnitude, frequency, and distribution.

5.1. Flood regime characteristics

According to gauge data, mean discharges range between 454 m³ s⁻¹ at Gangapur Dam (GD) and 2178 m³ s⁻¹ at Nandur Madmeshwar Dam (NMD) on the UGR (Fig. 1; Table 4). Historical and modern records show that large floods on the UGR occurred in 1939, 1965 (flood levels marked at Sarkarwada, an old administrative building of the 19th century, Nashik), 1969 (Mujumdar et al. 1970), 1976, 1979, 2004, 2005, 2006, 2008 (Khandare 2009), 2016, and 2019. The highest-ever recorded flood on the UGR at NMD in 1976 was on the order of 9977 m³ s⁻¹. This event, however, was not entirely natural. The unusually high discharge was primarily the result of a sudden release of a large volume of water from the dam. The second

largest flood of the UGB occurred on August 10, 2006, with gauged discharge of 8857 m³ s⁻¹ at Kopargaon (Fig. 1). The heaviest 24-hour rainfall, which occurred two days prior to the event, totaled 114 mm, or 9% (Table 3) of the annual rainfall. The other aspects of the UGR's flood regime are presented in the following section.

Table 4. Flood flow characteristics of the Upper Godavari River. Data source: CWC.

Sr. No.	River	Site	A (km²)	Record length	$Qmin$ (m³ s⁻¹)	$Qmax$ (m³ s⁻¹)	Qm (m³ s⁻¹)	Flood Range	$Qmax/Qm$
1	Godavari	Gangapur Dam (GD)	357	50	20	1886	454	1866	4.15
2	Godavari	Nashik	650	24	31	2288	481	2257	4.76
3	Godavari	Nandur Madmeshwar Dam (NMD)	1664	42	364	9977	2178	9613	4.58
4	Godavari	Chass	5230	25	160	5925	1212	5765	4.89
5	Godavari	Kopargaon	7096	27	128	8857	1822	8729	4.86
6	Darna	Darna Dam (DD)	404	41	142	1891	790	1749	2.39

$Qmin$ – minimum annual peak discharge; $Qmax$ – maximum annual peak discharge; Qm – mean annual peak discharge; A – catchment area. See Fig. 1 for the location of the sites.

5.1.1. Interannual variability in annual peak discharges

The temporal patterns of variability in the annual peak discharges at six sites on the UGB are shown in Figure 4. The graphs reveal high interannual variability in the annual peak discharges and the occurrence of one or two extreme events during the gauge period. A large amount of geomorphic work is accomplished by higher flows in the UGB. Floods that generate discharges several times greater than a river's mean flows are more likely to result in considerable geomorphic change (Kochel 1988). This effect can be established merely by estimating the $Qmax/Qm$ ratio. The $Qmax/Qm$ ratio for the UGB ranges from 2.39 to 4.89 (Table 4). Consequently, it can be concluded that maximum annual peak discharges ($Qmax$) are approximately five times larger than average peaks. The significance of higher discharges increases with flow variability (Wolman, Miller 1960). Such high flows are anticipated to have a significant impact on the geomorphic activities in the channel.

The coefficient of variation (Cv), which measures hydrological variability in annual peak discharges, is another useful indicator. The Cv, which ranges between 0.54 and 1.28 (Table 5), representing the ratio between the standard deviation (σ) and the mean (Qm), suggests moderate to high dispersion. The variability in flood flows may be credited to various hydrological events accountable for producing the floods.
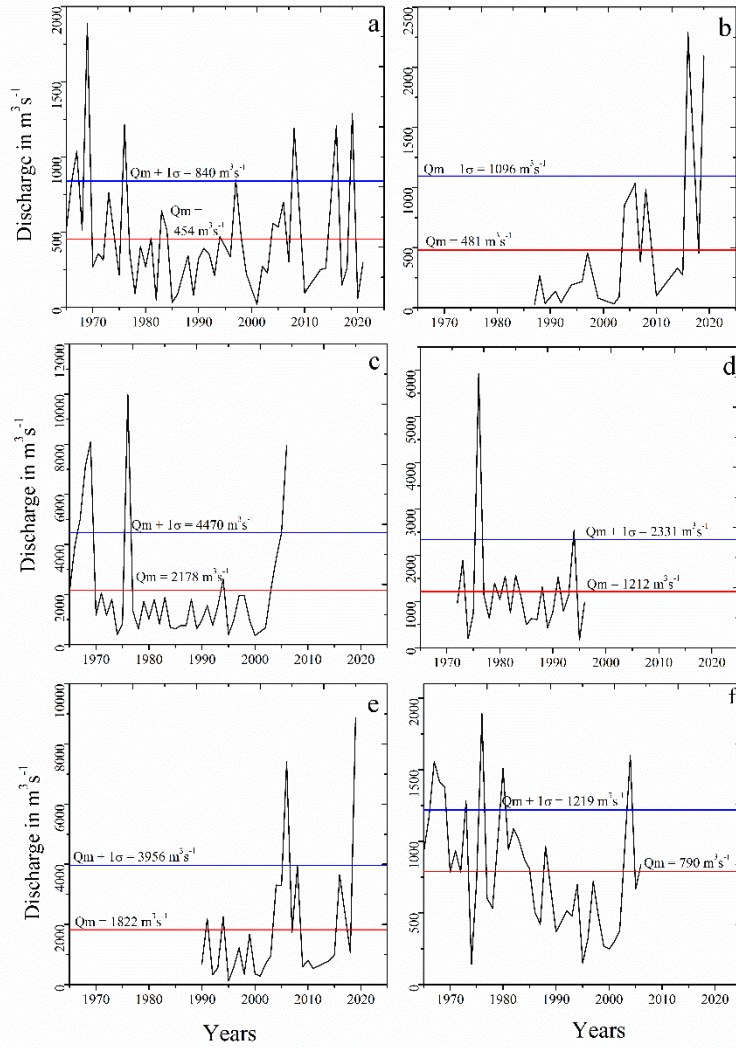
Fig. 4. Interannual variability in annual peak discharges, UGB: (a) Gangapur Dam, (b) Nashik, (c) Nandur Madmeshwar Dam, (d) Chass, (e) Kopargaon, (f) Darna Dam. See Fig. 1 for the location of the sites.

Table 5. Discharge characteristics of the UGB. Data source: CWC.

Sr. No.	River	Site	Record length	$Qmax$ (m³ s⁻¹)	Qm (m³ s⁻¹)	SD	Cv	Cs	Cs/Cv
1	Godavari	Gangapur Dam (GD)	50	1886	454	386	0.85	1.67	1.96
2	Godavari	Nashik	24	2288	481	615	1.28	2.0	1.56
3	Godavari	Nandur Madmeshwar Dam (NMD)	42	9977	2178	2292	1.05	2.07	1.97
4	Godavari	Chass	25	5925	1212	1119	0.92	3.34	3.62
5	Godavari	Kopargaon	27	8857	1822	2133	1.17	2.19	1.87
6	Darna	Darna Dam (DD)	41	1891	790	429	0.54	0.65	1.20

$Qmax$ – maximum annual peak discharge; Qm – mean annual peak discharge; SD – standard deviation; Cv – coefficient of variation; Cs – coefficient of skewness. See Fig. 1 for the location of the sites.

A number of researchers have used Beard's flash flood magnitude index ($FFMI$) to evaluate the variance in flood frequency as an index of the flashiness of floods (Baker 1977). The $FFMI$ values are calculated using the standard deviation of AMS logarithms, as mentioned below.

$$FFMI = \sqrt{\frac{\sum X^2}{N-1}}$$

(3)

where: X is $Xm - Qm$; Xm – annual maximum event; Qm – mean annual peak discharge; N – number of years of record (X, Xm, and Qm expressed as $\log_{10}$).

The $FFMI$ of the UGB ranges from 0.27 to 0.56, the mean $FFMI$ is 0.4 (Table 6). This $FFMI$ value is greater than the mean for the world, i.e., 0.28 (McMahon et al. 1992; Erskine, Livingstone 1999). The high mean $FFMI$ indicates that UGR floods are slightly more flashy and variable than the average for world rivers. The $FFMI$ further suggests a greater possibility for significant geomorphic changes during large floods.

Table 6. Flash flood magnitude indices ($FFMI$) of the Upper Godavari River. Data source: CWC.

Sr. No.	River	Site	Record length	$FFMI$
1	Godavari	Gangapur Dam (GD)	50	0.42
2	Godavari	Nashik	24	0.56
3	Godavari	Nandur Madmeshwar Dam (NMD)	42	0.37
4	Godavari	Chass	25	0.32
5	Godavari	Kopargaon	27	0.45
6	Darna	Darna Dam (DD)	41	0.27
7	UGB	Mean value	-	0.40

See Fig. 1 for the location of the sites.

5.1.2. Skewness

The coefficient of skewness (Cs) is the most common statistical moments employed in investigations of flood geomorphology and flood hydrology. Since the AMS data are not normally distributed, it is vital to find the Cs of the data. The values of Cs for all the stations on the UGR are positive, ranging from 0.65 to 3.34 (Table 5). The Cs values computed for other large rivers in India (Sakthivadivel, Raghupathy 1978; Hire 2000) are similar to the skewness values derived for the UGB. The positive Cs values predict the occurrence of one or two (or a few) very large magnitude flows during the gauge period. However, the characteristic of skewness is of doubtful value when applied to less than 50 years of data (Viessman et al. 1989). Subsequently, some hydrologists have also used the ratio Cs/Cv to further consolidate the degree of skewness (Shaligram, Lele 1978). The Cs/Cv ratio for different UGB discharge-gauging sites ranges from 1.20 to 3.62 (Table 5). The Cs/Cv ratios are often greater than 2.0 for the majority of India's large rivers (Shaligram, Lele 1978), demonstrating that peak discharge distribution is not extremely skewed.

5.1.3 Unit discharges (Q_u)

Unit discharge (Q_u) is a crucial indicator of the potential for large floods on a river (Gupta 1988). This ratio divides maximum annual peak discharge (Q_{max}) by the upstream catchment area (A), giving discharge or water yield per unit drainage area (m³ s⁻¹ km⁻²). The Q_u computed for all the sites on the UGB range from 1.13 to 6.00 m³ s⁻¹ km⁻² (Table 7). For the UGB as a whole, the Q_u is 3.64 m³ s⁻¹ km⁻². These unit discharges fall below the world envelope curve of the unit discharges constructed by Baker (1995). In comparison, the unit discharges of natural extreme floods on large peninsular rivers vary from 0.13 to 0.65 m³ s⁻¹ km⁻² (Kale et al. 1997; Hire 2000). In terms of geomorphic changes in the valley and channel, these discharges are likely to be effective (Costa, Connor 1995; Kale et al. 1997).

Table 7. Unit discharges (Q_u) of the Upper Godavari River. Data source: CWC.

Sr. No.	River	Site	A (km²)	Q_{max} (m³ s⁻¹)	Q_u (m³ s⁻¹ km⁻²)
1	Godavari	Gangapur Dam (GD)	357	1886	5.28
2	Godavari	Nashik	650	2288	3.52
3	Godavari	Nandur Madmeshwar Dam (NMD)	1664	9977	6.00
4	Godavari	Chass	5230	5925	1.13
5	Godavari	Kopargaon	7096	8857	1.25
6	Darna	Darna Dam (DD)	404	1891	4.68

A – catchment area; Q_{max} – maximum annual peak discharge. See Fig. 1 for the location of the sites.

6. Flood geomorphology

Flood geomorphology is concerned with the forms, processes, causes, and effects of floods (Baker 1988). Floods are primarily accountable for sculpting the river channel and the landscape in some hydro-geomorphic environments, for instance, the seasonal tropics (Wohl 1992; Gupta 1995). One of the significant themes in flood geomorphology has been the measurement and evaluation of the geomorphic efficiency of floods of various magnitudes. The geometry of river channels is considered to be a key factor in establishing the geomorphic effect of floods (Kochel 1988). To assess the geomorphic effects of floods, cross-sectional surveys were carried out at four sites (Fig. 5a-d) on the UGR to understand the channel geometry/morphology; hydraulic and hydrodynamic parameters of all the stations for respective high flood levels (HFL) have been computed and analyzed (Table 8).

The geomorphic efficacy of a flood, which relates to its capacity to affect the shape of the landscape (Wolman, Gerson 1978), is linked to flood power and the degree of turbulence (Baker, Costa 1987; Wohl 1993; Baker, Kale 1998; Kale, Hire 2004, 2007). Therefore, for identified unusual flood events, boundary shear stress (τ), stream power per unit boundary area (ω), Froude number (Fr) and Reynolds number (Re) were computed with the help of the following formulas (Equations 4 to 7) (Leopold et al. 1964; Baker, Costa 1987).

$$\omega = \gamma QS/w \tag{4}$$

$$\tau = \gamma RS \tag{5}$$

$$Fr = \overline{V}/(gR)^{0.5} \tag{6}$$

$$Re = \overline{V}R/v \tag{7}$$

where: ω is unit stream power expressed in watts per square meter (W m^{-2}); γ is the specific weight of clear water (9800 N m^{-3}); Q is discharge in m^3 s^{-1}; S is the slope, w is the water surface width in m; τ is the boundary shear stress expressed in Newtons per square meter (N m^{-2}); R is the hydraulic radius or mean depth of water in m. Fr – Froude number; $\overline{V}$ – mean flow velocity in m s^{-1}; g – acceleration due to gravity (9.8 m s^{-2}); Re – Reynolds number; v – kinematic viscosity (1×10^{-7} m^2 s^{-1} for water temperature of 20°C; Petts, Foster 1985).

Critical velocity for inception of cavitation (V_c) is another measure of the erosional power of flows (Equation 8). The V_c in m s^{-1} is given by Baker (1973) and Baker, Costa (1987).

$$V_C = 2.6\,(10 + D)^{0.5} \tag{8}$$

where V_c is the critical velocity for the inception of cavitation in m s^{-1} and D is flow depth.
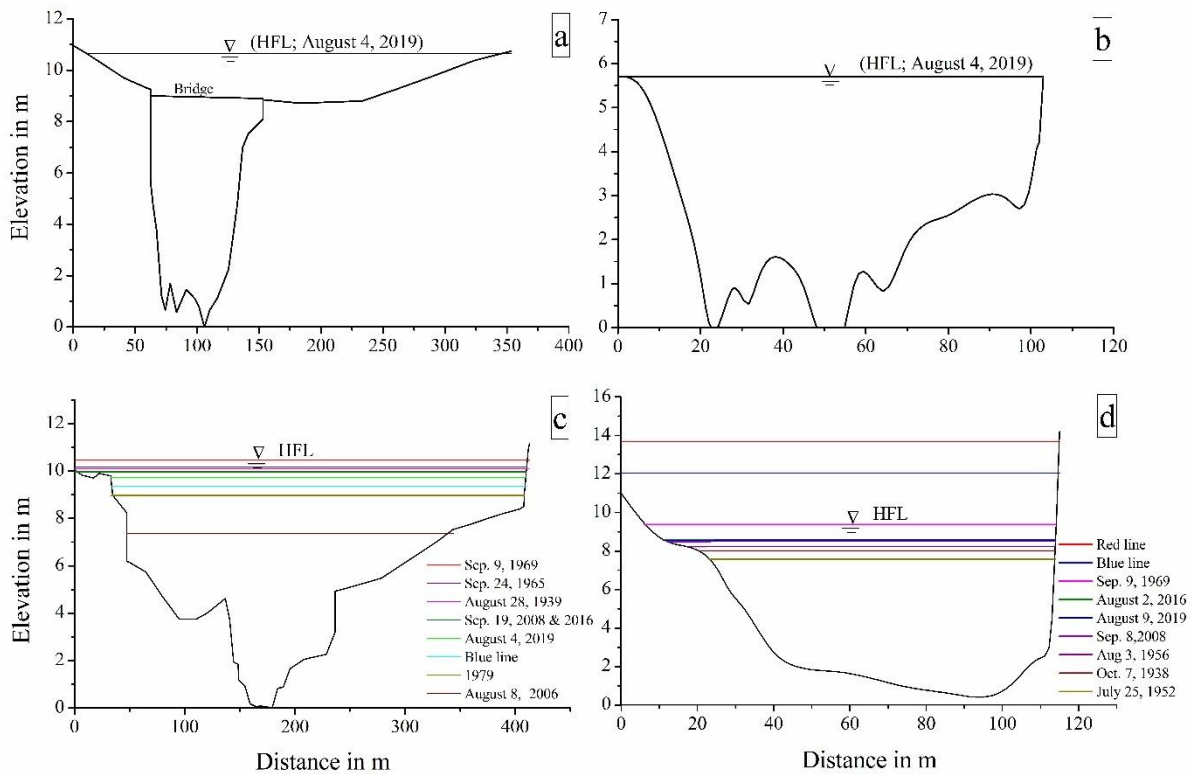

Fig. 5. Cross sections, UGR. (a) Dugaon, (b) Someshwar; (c) Sarkarwada; (d) Odha. See Fig. 1 for the location of sites. HFL – High flood level; Red line = 100-year flood line; Blue line = 25-year flood line.

Table 8. Hydraulic parameters of rare floods on the Upper Godavari River.

Sites on the UGR	DD.MM.YY	Discharge Q (m³ s⁻¹)	Width W (m)	Depth D (m)	Slope S	Velocity $\bar{V}$ (m s⁻¹)	Shear stress τ (N m⁻²)	Unit Stream Power ω (W m⁻²)	Fr	$Re×10^7$	Vc (m s⁻¹)
Dugaon	04.08.2019	1583	92	10.65	0.00357	3.12	192.48	600.71	0.43	17.17	11.81
Someshwar	04.08.2019	1894	101.81	5.20	0.012	5.17	423.36	2188	0.87	18.61	10.14
Sarkarwada	28.08.1939	2830.98	102.50	10.09	0.00423	3.97	288.21	1145.35	0.48	27.62	11.65
	24.09.1965	2878.76	102.50	10.16	0.00423	4.00	291.11	1164.68	0.48	28.09	11.67
	09.09.1969	3087.14	102.50	10.46	0.00423	4.11	303.55	1248.99	0.49	30.12	11.76
	1979	2104.96	102.50	9.86	0.00423	3.53	241.35	851.62	0.47	20.54	11.59
	08.08.2006	1410.81	102.50	7.36	0.00423	3.01	189.93	570.78	0.45	13.76	10.83
	19.09.2008	2736.39	102.50	9.95	0.00423	3.92	282.41	1107.08	0.48	26.70	11.61
	19.09.2016	2736.39	102.50	9.95	0.00423	3.92	282.41	1107.08	0.48	26.70	11.61
	04.08.2019	2577.25	102.50	9.71	0.00423	3.83	272.45	1042.70	0.48	25.14	11.54
Odha	07.10.1938	3836.03	87.50	7.50	0.0102	8.60	509.80	4382.28	1.22	43.84	10.88
	25.07.1952	3346.91	87.50	7.10	0.0102	8.14	469.81	3823.51	1.20	38.25	10.75
	03.08.1956	4091.94	87.53	7.80	0.0102	8.82	529.79	4673.03	1.22	46.75	10.97
	09.09.1969	6148.46	104.00	8.90	0.0102	9.69	609.76	5909.61	1.25	59.12	11.30
	03.08.1990	3346.91	87.50	7.10	0.0102	8.14	469.81	3823.51	1.20	38.25	10.75
	19.09. 2008	4587.00	89.50	8.00	0.0102	9.15	559.78	5123.09	1.24	51.25	11.03
	02.08.2016	4724.61	89.50	8.10	0.0102	9.26	569.77	5276.78	1.24	52.79	11.06
	04.08.2019	4724.61	89.50	8.10	0.0102	9.26	569.77	5276.78	1.24	52.79	11.06

Fr – Froude number; Re – Reynolds number; Vc – critical velocity for inception of cavitation.

The discharges for the unusual floods on the UGR range from 1410 to 6148 m³ s⁻¹ (Table 8). These are large rainfall-runoff floods calculated by indirect methods. From the reconstructed hydraulic data, the stream power per unit area of the UGB ranges from 571 to 5909 W m⁻². In comparison, the estimated average unit stream power at a cross-section (alluvial) varies between 322 W m⁻² on the Godavari and less than 10 W m⁻² on the Brahmaputra (Kale 1998). Estimation of boundary shear stress for large floods by using Equation (5) indicates that the values for UGR range from 192 to 610 N m⁻² (Table 8). The estimated values for the Ganga, Yamuna, and Kosi Rivers are 11-25 N m⁻², and for the Narmada and Godavari Rivers (as a whole), the shear stress values are >50 N m⁻² (Kale, Gupta 2001). Floods generating shear stress of 10 N m⁻² can entrain and transport sediments of about 1 cm and can carry sediments finer than 1 mm in suspension (Komar 1988). The high values of shear stress on the UGR reflect the uncommonly high capacity of the river to entrain and transport coarse sediments.

The analysis further indicates that Froude numbers greater than 1 (supercritical flow) have occurred on the UGR at the deep, narrow bedrock reach at Odha (Fig. 1) for all the flow conditions (Table 8). Intense bedrock scouring, resulting from cavitating flow, is also reflected in erosional features such as polished

rock surfaces and potholes (Baker et al. 1988; Kale et al. 1993, 1994) at Odha ($Fr > 1$) and Someshwar sites ($Fr \approx 1$). High values of Reynolds numbers signify that the flood discharges could be exceedingly turbulent, and, therefore, capable of a variety of geomorphic actions. The Odha site (Fig. 1) produced the highest Reynolds number (59.12×10^7) for the September 1969 flood (Table 8), thus, it is probable that this reach experienced very intensive bedrock erosion. The critical velocity for the inception of cavitation (V_c) is a related measure of the erosional power of flows. According to estimates of V_c, no floods have ever exceeded the conditions described by Equation 8 at any of the survey sites on the UGR. However, erosional features, including flute marks, polished rock surfaces, and potholes at various locations at other sites on the UGR, are evidence of severe bedrock scouring by cavitating flow.

The channel bed of the UGR in alluvial reaches is composed of pebbly-cobbly gravel, and of boulders at the Dugaon site (Fig. 1). The sediment-transport equations developed by Williams (1983) were applied to determine the theoretical minimum critical values of bed shear stress (τ), unit stream power (ω), and mean velocity ($\overline{V}$) that could initiate cobble and boulder movement (Table 8). The equations used in the boulder transport calculations are as follows:

$$\omega = 0.079 \, dg^{1.27} \tag{9}$$

$$\tau = 0.17 \, dg \tag{10}$$

$$\overline{V} = 0.065 \, dg^{0.5} \tag{11}$$

where dg is the intermediate diameter of the grain in mm.

Theoretical estimates indicate that the unit stream power required for moving pebbles (4-64 mm), cobbles (64-256 mm), and a boulder (550 mm) is respectively 16, 90, and 239 W m^{-2}. The corresponding values of boundary shear stress are 11, 44, and 94 N m^{-2} (Williams 1983). A comparison of these theoretical estimates with the calculated values given in Table 9 specifies that, even though sand and pebbles are moved during all flows, floods on the UGR are capable of transporting cobble-sized sediments, and most of the large floods can move large boulders >550 mm in diameter. For instance, a concrete slab of bridge with i-axis of 810 mm was detached by the August 4, 2019 flood, with an estimated discharge of 2577 m^3 s^{-1} (Table 8) on the UGR at Sarkarwada (Fig. 1). This event produced unusually high values of bed shear stress (272 N m^{-2}), unit stream power (1043 W m^{-2}), and mean velocity (3.83 m s^{-1}) relative to the theoretical threshold estimates (Fig. 6, Table 9).

Further, the data computed for maximum velocities at Dugaon and Odha range from 3.12 to 9.69 m s^{-1} (Table 8), respectively. The maximum surface velocities for very large floods are not available. Nevertheless, for the September 1969 flood, the maximum surface velocity was recorded as 2.47 m s^{-1} at Paithan (Mujumdar et al. 1970), located in an area of gentle channel slope about 215 km downstream from Odha. According to available data, maximum velocities are much higher than the threshold velocities required

for the movement of coarse sediment. It is, therefore, certain that large amounts of coarse sediment are moved during large floods, surpassing the total amount of suspended load transported by moderate flows.

Fig. 6. A view of UGR upstream of Sarkarwada (See location in Fig. 1) on 5th August 2019 (a day after the August 2019 flood). Width of flow 128 m and depth of flow 9.71 m (Photograph taken from Holkar/Victoria Bridge, Nashik).

Table 9. Boulder dimensions at the Dugaon site and the associated theoretical entrainment values.

Site	Distance from source (km)	I-axis (mm)	$\bar{V}$ (m s^{-1})	τ (N m^{-2})	ω (W m^{-2})	W/D ratio
Dugaon	30	550	1.6	93.5	239	16.57
Panchvati (Sarkarwada)	44	810 (Concrete slab)	5.1	405	1535	39.12

ω – unit stream power in W m^{-2}; τ – boundary shear stress in N m^{-2}; $\bar{V}$ – mean velocity in m s^{-1}; W/D – width/depth ratio (August 4, 2019 flood).

7. Conclusions

The southwest summer monsoon (mid-June to early October) dominates the rainfall supply of the UGB by producing about 90% of the annual rainfall. Therefore, the annual flow pattern of the UGB is intimately coupled with the patterns of variation in summer monsoon rainfall. The LPS that originate predominantly over the Bay of Bengal boost the magnitude of rainfall and subsequent floods. Human interference, by releasing large volumes of water from the dams, also underlies changes in flow regimes of the UGB. The study further indicates that the interannual variability of rainfall was associated with increased frequency and magnitude of floods, primarily after the 1930s. High interannual variability persists in the annual peak discharges. The more variable the flow, the more significant the higher discharges become. The maximum annual peak discharges of the UGR are five times higher than average peaks. Therefore, geomorphic activity in the channel is likely to be vital. The slightly flashy and variable nature of floods on the UGR substantiates the possibility of the river experiencing significant geomorphic reworking during large floods. However, unit discharges of the UGR as a whole fall below the world envelope curve of unit

discharges constructed by (Baker 1995). The UGR shows high spatial variability in terms of flood hydraulics and hydrodynamics. The higher values for unit stream power and boundary shear stress for rare floods reveal the uncommonly high capacity of the river to erode and transport coarse sediments. The approximate Froude numbers for two sites, as expected, are less than 1, representing that the flows were mainly subcritical. However, Froude numbers >1 for the constricted reach of the bedrock channel at Odha for numerous flood stages revealed that the flows were supercritical. High Reynolds numbers indicate that the flood discharges could be exceedingly turbulent and, therefore, capable of accomplishing a variety of geomorphic activities. According to estimates of the values of critical velocity for the inception of cavitation (V_c), none of the intense floods on the UGR exceeded the conditions required for inception of cavitation. However, erosional features, including flute marks, polished rock surfaces, and potholes at several locations at other sites of the UGR and its tributaries, suggest intense bedrock scouring resulting from cavitating flow conditions. Theoretical estimates of unit stream power, bed shear stress and mean velocity coupled with transported large boulders indicate that the floods on the UGR are competent to move large boulders. The effectiveness of large-magnitude flood events is also evident from the presence of deep, narrow gorges, scablands, polished rock surfaces, inner channels, and waterfalls at several locations on the UGR.

Acknowledgments

References

Abbi S.D.S., Jain B.C., 1971, A study of major rainstorms of Tapi basin for evaluation of design storm, MAUSAM, 22 (4), 203-212, DOI: 10.54302/mausam.v22i2.4483.

Anwat V., 2022, Fluvial and Flood Geomorphological Investigations of Bedrock Channel Reaches of The Damanganga River, Ph.D. Thesis, Savitribai Phule Pune University, Pune, 225 pp.

Baker V.R., 1973, Erosional forms and processes for the catastrophic Pleistocene Missoula floods in eastern Washington, [in:] Fluvial Geomorphology, M. Morisawa (ed.), 123-148

Baker V.R., 1977, Stream-channel response to floods, with examples from central Texas, Bulletin of the Geological Society of America, 88 (8), 1057-1071, DOI: 10.1130/0016-7606(1977)88<1057:SRTFWE>2.0.CO;2

Baker V.R., 1988, Flood erosion, [in:] Flood Geomorphology, V.R. Baker, R.C. Kochel, P.C. Patton (eds.), Wiley, New York, 81-95.

Baker V.R., 1995, Global paleohydrological change, Quaestiones Geographicae, 4, 27-35.

Baker V.R., Costa J.E., 1987, Flood power, [in:] Catastrophic Flooding, V.R. Baker, J.E. Costa (esd.), Routledge, 1-21.

Baker V.R., Kale V.S., 1998, The role of extreme floods in shaping bedrock channels, [in:] Rivers Over Rock: Fluvial Processes in Bedrock Channels, Geophysical Monograph Series, 107, American Geophysical Union, Washington, D.C., 153-165, DOI: 10.1029/GM107p0153.

Costa J., Connor J.O., 1995, Gemorphologically effective foods, [in:] Natural and Anthropogenic Influences in Fluvial Geomorphology, Geophysical Monograph, 89, American Geophysical Union, 45-56.

Dhar O.N., Kulkarni A.K., Mandal B.N., 1984, The most severe rainstorm of india – a brief appraisal, Hydrological Sciences Journal, 29 (2), 219-229, DOI: 10.1080/02626668409490935.

Dhar O.N., Nandargi S., 1995, On some characteristics of severe rainstorms of India, Theoretical and Applied Climatology, 50, 205-212, DOI: 10.1007/BF00866117.

Erskine W.D., Livingstone E., 1999, In-channel benches: the role of floods in their formation and destruction on bedrock confined rivers, [in:] Varieties of Fluvial Form, A.J. Miller, A. Gupta (eds.), John Wiley and Sons, 445-475.

Gupta A., 1988, Large floods as geomorphic events in the humid tropics, [in:] Flood Geomorphology, V.R. Baker, R.C. Kochel, PC. Patton (eds.), John Wiley and Sons, NY, 301-320.

Gupta A., 1995, Magnitude, frequency, and special factors affecting channel form and processes in the seasonal tropics, [in:] Natural and Anthropogenic Influences in the Fluvial Geomorphology, Geophysical Monograph Series, 89, American Geophysical Union, 125-136.

Hire P.S., 2000, Geomorphic and Hydrologic Studies of Floods in Tapi Basin, Ph.D. Thesis, University of Pune, Pune (India), 192 pp.

Kale V., Gupta, A., 2001, Introduction to Geomorphology, Introduction to Geomorphology. Orient Longman, New Delhi, 274 pp.

Kale V., Mishra S., Enzel Y., Ely L., Rajaguru S.N., Baker V.R., 1993, Flood geomorphology of the Indian Peninsular rivers, Journal of Applied Hydrology, 6, 49-55.

Kale V.S., 1998, Monsoon floods in India: a hydro-geomorphic perspective, Memoir Geological Society of India, 41, 229-259.

Kale V.S., 1999, Long-period fluctuations in monsoon floods in the Deccan Peninsula, India, Journal of Geological Society of India, 53, 5-15.

Kale V.S., 2022, Holocene regional-scale behavior of the rivers of Indian Peninsula, [in:] Holocene Climate Change and Environment, N. Kumaran, P. Damodara (eds.), Elsevier, 103-129, DOI: 10.1016/B978-0-323-90085-0.00017-6.

Kale V.S., Ely L.L., Enzel Y., Baker V.R., 1994, Geomorphic and hydrologic aspects of monsoon floods on the Narmada and Tapi Rivers in central India, Geomorphology (1-4), 10, 157-168, DOI: 10.1016/0169-555X(94)90014-0.

Kale V.S., Hire P., Baker V.R., 1997, Flood hydrology and geomorphology of monsoon-dominated rivers: The Indian Peninsula, Water International, 22 (4), 259-265, DOI: 10.1080/02508069708686717.

Kale V.S., Hire P.S., 2004, Effectiveness of monsoon floods on the Tapi River, India: Role of channel geometry and hydrologic regime, Geomorphology, 57 (3-4), 275-291, DOI: 10.1016/S0169-555X(03)00107-7.

Kale V.S., Hire P.S., 2007, Temporal variations in the specific stream power and total energy expenditure of a monsoonal river: The Tapi River, India, Geomorphology, 92 (3-4), 134-146, DOI: 10.1016/j.geomorph.2006.06.047.

Khandare P.R., 2009, Spatio-temporal aspects of floods on the Godavari River in the Nashik District, MPhil Thesis, Yashwantrao Chavan Maharashtra Open University, Nashik, 131 pp.

Kochel R.C., 1988, Geomorphic impact of large floods: review and new perspectives on magnitude and frequency, [in:] Flood geomorphology, V. Baker, R. Kochel, P. Patton (eds.), John Wiley and Sons, New York, 169-187.

Komar P.D., 1988, Sediment transport by floods, [in:] Flood Geomorphology, V.R. Baker, R.C. Kochel, P.C. Patton (eds.), Wiley, New York, 97-112.

Leopold L.B., Wolman M.G., Miller J.P., 1964, Fluvial Processes in Geomorphology, 2nd edition, Dover Publications, 522 pp.

McMahon T.A., Finlayson B.L., Haines A.T., Srikanthan R., 1992, Global runoff: continental comparisons of annual flows and peak discharges, Catena Verlag, 166 pp.

Mooley D.A., 1973, Some aspects of Indian monsoon depressions and the associated rainfall, Monthly Weather Review, 101, 271-280, DOI: 10.1175/1520-0493(1973)101<0271:saoimd>2.3.co;2.

Mujumdar G.G., Rajaguru S.N., Pappu R.S., 1970, The recent Godavari flood (September 1969) and its relevance to prehistoric archaeology, Bulletin of the Deccan College Post-Graduate and Research Institute, 29 (1-4), 118-134.

Pandharinath N., 1984, A case study of 1981 flood in the Godavari River, MAUSAM, 35 (2), 195-198, DOI: 10.54302/MAUSAM.V35I2.2004.

Pant G.B., Kumar K.R., 1997, Climates of South Asia, Belhaven Studies in Climatology, Wiley, 280 pp.

Patil A., Hire P., 2020, Flood hydrometeorological situations associated with monsoon floods on the Par River in Western India, MAUSAM, 71 (4), 687-698, DOI: 10.54302/mausam.v71i4.58.

Patil A.D., 2018, Bedrock Channel of the Par River : Its Forms and Processes, PhD Thesis, Tilak Maharashtra Vidyapeeth, Pune, 253 pp.

Pawar U.V, Hire P.S., 2018, Long term fluctuations and global teleconnections in the monsoonal rainfall and associated floods of the Mahi Basin: Western India, International Journal of Scientific and Technology Research, 5 (1), 237-242.

Pawar U.V., 2019, An Analytical Study of Geomorphological, Hydrological, and Meteorological Characteristics of Floods in the Mahi River Basin: Western India, PhD Thesis, Tilak Maharashtra Vidyapeeth, Pune, 211 pp.

Petts G.E., Foster I.D.L., 1985, Rivers and Landscape, Edward Arnold, London, 274 pp.

Ramaswamy C., 1987, Meteorological Aspects of Severe Floods in India 1923-1979, Meteorological Monography: Hydrology, No. 10, India Meteorological Department, 400 pp.

Sakthivadivel R., Raghupathy A., 1978, Frequency analysis of floods in some Indian rivers, Hydrology Review, 4, 57-67.

Shaligram V.M., Lele V.S., 1978, Analysis of hydrologic data using Pearson type III distribution, Hydrology Research, 9 (1), 31-42, DOI: 10.2166/nh.1978.0004.

Viessman W., Lewis G.L., Knapp J.W., 1989, Introduction to Hydrology, Harper and Row, New York, 612 pp.

Williams G.P., 1983, Paleohydrological methods and some examples from Swedish fluvial environments I, Cobble and boulder deposits, Geografiska Annaler: Series A. Physical Geography, 65 (3-4), 227-243, DOI: 10.1080/04353676.1983.11880088.

Wohl E.E., 1992, Bedrock benches and boulder bars: floods in the Burdekin Gorge of Australia, Geological Society of America Bulletin, 104 (6), 770-778, DOI: 10.1130/0016-7606(1992)104<0770:BBABBF>2.3.CO;2.

Wohl E.E., 1993, Bedrock channel incision along Piccaninny Creek, Australia, Journal of Geology, 101 (6), 749-761, DOI: 10.1086/648272.

Wolman M.G., Gerson R., 1978, Relative scales of time and effectiveness of climate in watershed geomorphology, Earth Surface Processes, 3 (2), 189-208, DOI: 10.1002/esp.3290030207.

Wolman M.G., Miller J.P., 1960, Magnitude and frequency of forces in geomorphic processes, Journal of Geology, 68 (1), 54-74, DOI: 10.1086/626637.